CF_4 on Carbon Nanotubes: Physisorption on Grooves and External Surfaces

Luke Heroux, Vaiva Krungleviciute, M. Mercedes Calbi, and Aldo D. Migone*

Department of Physics, Neckers 483A, Southern Illinois University, Carbondale, Illinois 62901-4401

Received: February 14, 2006; In Final Form: April 7, 2006

We present the combined results of a computer simulation and adsorption isotherm investigation of CF_4 films on purified HiPco nanotubes. The experimental measurements found two substeps in the adsorption data. The specific surface area of the sample and the coverage dependence of the isosteric heat of adsorption of the films were determined from the measurements. The simulations, conducted for homogeneous bundles of close-ended tubes, also found two substeps in the first layer data: one corresponding to adsorption on the grooves and a second one, at higher pressures, corresponding to adsorption on the outside surface of the tubes. Our computer simulations are in very good agreement with the experimental data.

1. Introduction

Films adsorbed on bundles of carbon nanotubes have attracted the attention of researchers in experiments, computer simulations, and theory, ever since nanotubes were produced in sufficient quantities to make adsorption studies feasible.[1−3] A problem of considerable importance in adsorption is that of determining where on the nanotube bundles the gas molecules adsorb.[4−16] This problem has implications for practical applications (e.g., for determining the upper limit of the gas storage capacity of nanotubes[17,18]), and it is also relevant from a fundamental perspective (e.g., for determining whether quasi-one-dimensional phases can be formed, via adsorption, on carbon nanotubes).[19−29]

Theoretically there are three possible groups of adsorption sites on bundles of close-ended single-walled carbon nanotubes (SWNTs): interstitial channels (ICs), grooves, and the outer surface sites of individual tubes on the periphery of the bundles.[7] For open-ended tubes the interior of individual tubes constitutes a fourth group of sites.[7] Access to each group of adsorption sites is determined by the size of the adsorbate, the size of the nanotubes forming the bundles, the degree of homogeneity of the bundles, and the presence or absence of chemical compounds blocking access to the sites.[7,16,25,26]

Experimentally, monolayer adsorption isotherms of rare gases and small simple molecules display two broad substeps.[1,5,9] The explanation for the origins of these substeps is still the subject of some controversy.[4−15] It is widely agreed, however, that the higher pressure (weaker binding) susbtep is a manifestation of adsorption on the outer surface sites of individual tubes located on the periphery of a bundle.[1,5] The lower pressure (stronger binding) substep has been variously attributed to adsorption on the grooves,[4] to adsorption in the interstitial channels,[11] to a combination of adsorption on the grooves and in the wider interstitial channels present in inhomogeneous bundles,[9,16] or to adsorption at the interior of open-ended tubes.[10,12]

CF_4 is an effectively spherical molecule which consists of a central carbon atom surrounded by four fluorine atoms. It has a molecular area of 18.9 Å^2, a value slightly larger[31] than that of Xe. The interactions between CF_4 molecules are stronger than those for most of the other species that have been used in adsorption studies on nanotubes.[7] As a result, CF_4 films have some potential for exhibiting behavior not seen with smaller, weaker adsorbates on nanotube bundles.

Adsorption by CF_4 on the inside and outside of bundles of single-walled carbon nanotubes has been studied using adsorption isotherms,[5] infrared spectroscopy,[32,33] and computer simulations.[32,33] The possibility that CF_4 films may exhibit unusual behavior appeared to be confirmed in an adsorption isotherm study.[5] This study found only one broad substep present (the lower binding/higher pressure one) in the first layer data for CF_4. To explain the absence of the higher binding substep, the authors suggested that the CF_4 molecules are too large to feel the corrugation in the substrate potential that produces the grooves[5] (i.e., that the CF_4 molecules do not experience the grooves as distinct sites). In direct contrast to this explanation, the results of a spectroscopic study of CF_4 on SWNTs were interpreted in terms of adsorption on the grooves.[32,33] Unlike the isotherm study, which explored full monolayer coverages, the spectroscopic study investigated fairly low values of the pressure and of the coverage.[32]

Here we present the results of a thermodynamic and computer simulation study of the adsorption of CF_4 on bundles of SWNTs. The analysis resulting from combining our experimental and simulation results for this molecule, in addition to addressing the differences found in previous studies of this system, allows us to arrive at some general conclusions regarding the nature of the nanotube bundles and of the adsorption process on them.

2. Experimental Measurements

In our measurements we used Research Purity CF_4 gas produced by Matheson Tri-Gas. The gas was used without any further purification.

The substrate used in these experiments was HiPco purified single-walled carbon nanotubes, from Batch No. CM26-0026-1, produced by CNI.[34] These nanotubes were purified by the manufacturer; the nanotubes used had a reported purity of 91%.[35] Nanotubes resulting from the HiPco process arranged into bundles that ranged from 10 to1000 tubes per bundle; however, most of the bundles in our sample were expected to have between 10 and 40 tubes.[35] The average diameter of the tubes was 1 ± 0.2 nm (this is slightly narrower than the typical

* Corresponding author. Phone: (618) 453-1053. Fax: (618) 453-1056. E-mail: aldo@physics.siu.edu.

10.1021/jp060956h CCC: $33.50
Published on Web 06/07/2006

TABLE 1: Lennard-Jones Parameters Used To Describe Gas−Gas and Gas−Surface Interactions[a]

σ_{gg} (Å)	ϵ_{gg} (K)	σ_{gs} (Å)	ϵ_{gs} (K)
4.58	157	3.99	66.3

[a] Combining rules were applied with $\sigma_{CC} = 3.4$ Å and $\epsilon_{CC} = 28$ K for the corresponding carbon−carbon interactions.

nanotubes produced by arc discharge).[35] The weight of the sample used in these experiments was 0.334 g.

The nanotube sample was placed in a copper-gasketed stainless steel cell and heated at 300 °C under 10^{-4} Pa pressure for a period of 3 h. After this heating period, a valve to the cell was closed, and the cell was transported and connected to the adsorption setup, while the contents of the cell were maintained under vacuum. The setup was evacuated before the valve to the cell was reopened. Prior to each isotherm, the entire setup, including the sample, was pumped for no less than 2 days to a pressure on the order of 10^{-4} Pa, or lower.

The measurements were performed in an in-house built, automated adsorption apparatus. The pressures were determined using MKS capacitance pressure transducers having maximum pressure ranges of 1, 100, and 1000 Torr. The dosing volume was at room temperature. The cell containing the nanotubes substrate was mounted on top of a cryogenic cold-head. All of the equipment was attached to an IBM-compatible PC through GPIB and PCI connections. A program, developed in our laboratory using LabVIEW, controlled the opening and closing of the automated valves, established the shot size, and determined that the equilibrium condition was met. The program also calculated the amount of gas adsorbed.

3. Theoretical Calculations

Grand canonical Monte Carlo simulations were performed to explore CF_4 adsorption on the external surface of the bundle. This study provides detailed information on the evolution of adsorbed phases as a function of temperature and/or external pressure. The results can be directly compared with the experimental measurements. In the past, we have used a similar approach to extensively study the structure of phases (Ne, Ar, Kr, CH_4, Xe) adsorbed on carbon nanotubes.[28−30] Our predictions have been found to be in agreement with results of different adsorption experiments.[1,19,21,29,30]

Since the experimental sample is expected to have the interior spaces of the majority of the tubes inaccessible for adsorption (the ends of the tubes being either capped or blocked), and since the *nondefect* interstices between the tubes are too small to accommodate this large molecule, we limited the simulations to adsorption on the exterior of the bundle (see discussion below).

We model the adsorbent surface by lining up parallel tubes with the same radii ($R = 5$ Å), as we have done in previous work.[28,29] The wall-to-wall separation between the tubes is assumed to be 3.2 Å. As done in previous adsorption studies of CF_4 on nanotube bundles,[32] we consider this molecule as a spherical adsorbate, neglecting its internal degrees of freedom. While the specific internal structure of the molecule may play an important role in determining the structure of solid phases at very low temperature, we do not expect to find any significant effects on the phases investigated here at temperatures higher than 100 K. The agreement found a posteriori with the experimental results gives support to this assumption. The gas−surface (gs) and gas−gas (gg) interactions are based on Lennard-Jones pair potentials using the parameters given in Table 1 and semiempirical combining rules.[7]

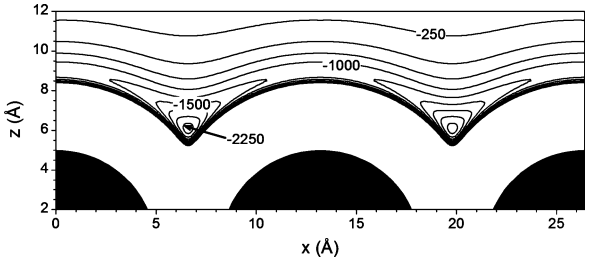

Figure 1. Potential energy (in K) of a CF_4 molecule near the external surface of a nanotube bundle in the simulation cell. The dark regions at the bottom of the panel correspond to space occupied by the tubes.

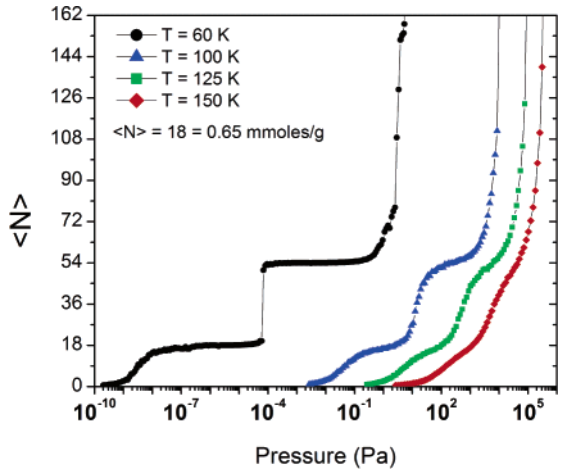

Figure 2. Adsorption isotherms of CF_4 on the exterior of the bundle from computer simulations. From left to right, the curves correspond to temperatures of 60, 100, 125, and 150 K.

Figure 1 shows the resulting potential energy that a CF_4 molecule feels in the vicinity of the external surface of the tubes. That potential is derived by summing the contribution of carbon atoms from two adjacent tubes.[7] The simulation cell has a length of 26.4 Å along the *x*-direction (twice the distance between the axis of two adjacent tubes) and $10\sigma_{gg}$ along the axis of the tubes (*y*-direction). Periodic boundary conditions were used for these two directions. The height of the cell along the *z*-direction (pointing away from the surface) is set to 40 Å. The details of this calculation and the simulation method have been described in earlier studies.[28]

At fixed temperature, the equilibrium coverage is calculated as a function of the external pressure of the gas to produce the set of isotherms shown in Figure 2. The amount of gas adsorbed is given as the average number of molecules $\langle N \rangle$ per unit cell. Since the length of the cell along the tubes' axis is $10\sigma_{gg}$, $\langle N \rangle = 9$ for any closed-packed line of molecules that lies along the *y*-direction. One may convert this coverage scale to commonly used coverage units if the geometry of the bundle is specified. For instance, assuming that a typical bundle contains 37 tubes (with 18 external grooves), the groove phase coverage $\langle N \rangle = 18$ would be equivalent to 0.65 mmol of adsorbate per gram of carbon.

As was found for other gases adsorbing on the external surface of a bundle, the isotherms show a series of steps corresponding to the completion of different phases in the adsorbed film as the pressure is increased. The lowest temperature isotherm ($T = 60$ K) allows the easiest characterization of the structure of the phases. Adsorption begins with the formation of the groove phase (first plateau at $\langle N \rangle = 18$ since the cell contains two grooves), followed by monolayer completion that consists of two more lines of CF_4 molecules symmetrically adsorbed at each side of the grooves ($\langle N \rangle = 54$).

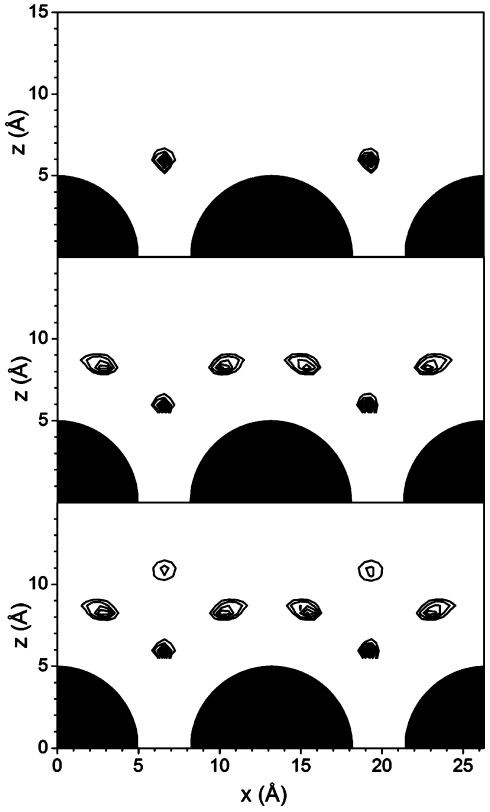

Figure 3. CF_4 density contours at $T = 100$ K for increasing values of the coverage (pressure). From top to bottom: groove phase ($P = 2.5$ Pa, $\langle N \rangle = 18$); monolayer phase ($P = 284$ Pa, $\langle N \rangle = 54$); second groove phase ($P = 3545$ Pa, $\langle N \rangle = 70$).

These first two steps are the main features of the isotherms and are easily identified in isotherms up to around 180 K. The $T = 60$ K isotherm shows that further increase in the pressure leads to the formation of another groove phase in the second layer. The completion of the second layer ($\langle N \rangle = 99$) is not distinguishable, and the pressure step ends up with the plateau that indicates the formation of the third layer. As expected, these higher coverage features are not resolvable in higher temperature isotherms.

Figure 3 illustrates the evolution of the density of the adsorbed film as the coverage (pressure) increases at $T = 100$ K. The formation of the groove and the monolayer phases is clearly identified. Even though the corrugation of the potential is significantly reduced after monolayer completion, a second groove phase is still observable. Further increase in the pressure produces the adsorption of a bulk-like film where even the multilayer transitions are not noticeable due to the reduction in the variation of the potential away from the nanotube surface. This rapid loss of corrugation in the potential is a direct consequence of the large size of the adsorbate.

4. Results and Discussion

Adsorption Sites and Surface Area Determinations. Our adsorption isotherm measurements were divided into two groups: we conducted low-coverage measurements (less than one-third of a monolayer) for temperatures between 175 and 207 K, and we performed full monolayer isotherms for temperatures between 101 and 138 K. For reference, the bulk triple point of CF_4 is 89.5 K.

The specific surface area of the sample was determined using the so-called "point B" method[36] (see Figure 4). Taking the molecular area of CF_4 to be 18.9 Å^2 and using a monolayer

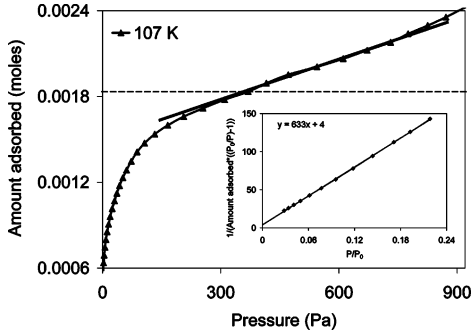

Figure 4. Adsorption isotherm at 107 K (plotted on a linear scale) used to determine specific surface area via the point B method. The dashed line indicates the coverage at monolayer completion. The inset displays the BET plot corresponding to the isotherm data.

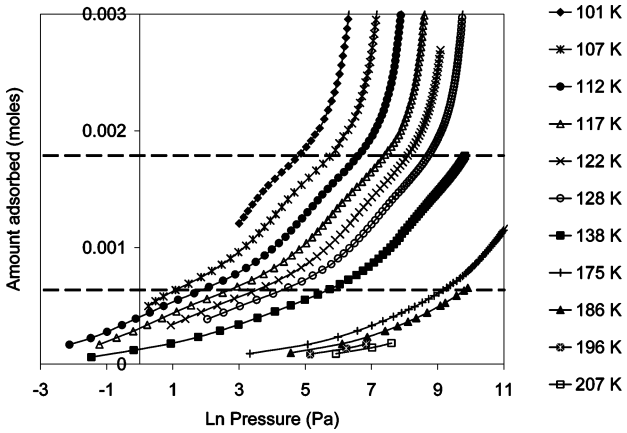

Figure 5. Complete set of adsorption isotherms measured in this work. The upper dashed line indicates monoloyer completion (see Figure 4); the lower dashed line corresponds to the top of the lower pressure substep.

completion value of 1.768 mmol, we obtained a specific surface area for this sample of 602 m^2/g. This result is in excellent agreement with the value for the specific area found using Xe isotherms, for another sample of this same batch of nanotubes (we found a value of 608 m^2/g from the Xe data).[37]

For comparison with a more commonly used method for determining the specific surface area, we applied the BET equation[38] to our data (inset in Figure 4). The BET value for the area is 535 m^2/g, in reasonably good agreement with the point B value for this quantity. We note that when one compares the simulations (where layer completion can be very clearly determined at low temperatures) with the experimental results (where monolayer completion is somewhat more ambiguous) it is clear that for this system the point B method provides a closer match to the monolayer completion obtained in the simulations.

Full monolayer isotherms were conducted to search for the presence of features in the first layer data. For most of the isotherms measured in this group we used small coverage intervals (on the order of 0.03 layer) between data points. A semilogarithmic plot of the isotherms in this group is presented in Figure 5. Close inspection of the curves in this figure, especially of the five between isotherms 107 and 122 K, reveals the presence of two substeps in the first layer data.

The higher pressure step, which is the most clearly visible feature in the data, corresponds to adsorption on the outer surface of individual tubes in the periphery of the bundle. As we discuss in greater detail below, a comparison with our computer simulation results shows that the lower coverage substep is most

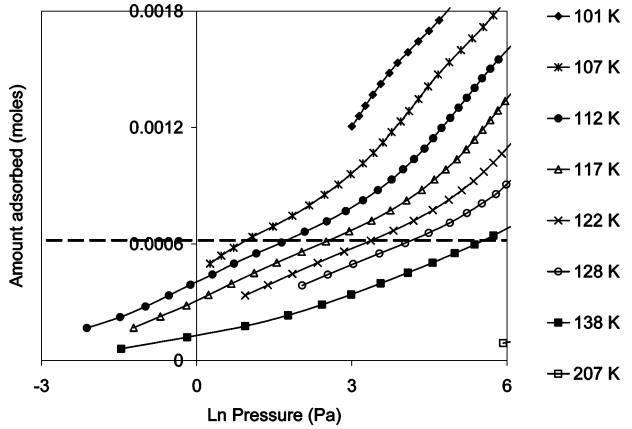

Figure 6. Expanded view of the low-coverage region for the low-temperature isotherms shown in Figure 5. The dashed line indicates the top of the lower pressure substep.

likely due to adsorption on the grooves. An expanded view of the data corresponding to the lower coverage substep is shown in Figure 6. The coverage at the top of this substep corresponds to approximately 34% of the monolayer completion value.

The previous adsorption isotherm study of CF_4 (which investigated three isotherms in the vicinity of 100 K) found only a single step in the first layer data.[5] This step was identified as corresponding to adsorption on the outer surface of the individual tubes at the periphery of the bundle. The isosteric heat corresponding to that single isotherm feature was 0.8 times the value of that for CF_4 on planar graphite.[5] The authors of that adsorption study argued that steric hindrance resulted in the absence of a lower pressure substep for Freon. That is, the large diameter of the CF_4 molecule prevents it from experiencing the corrugation in the substrate potential present on the periphery of the bundle (it is this corrugation that gives rise, in the case of smaller adsorbates, to separate isotherm features and to higher binding energies for adsorption on the grooves relative to adsorption on the outer surface sites). Their interpretation was also supported by a comparison of the specific surface area determined with CF_4, CH_4, and Xe: the study found that for CF_4 the specific area was approximately 86% of the value determined with either Xe or methane adsorption; steric hindrance was again the explanation offered for this observation.

Why is it that we have found a substep in a regime where previous measurements failed to find one? In each of the three isotherms performed in that study, there were no more than three data points taken in the lower fourth of the first layer, i.e., in the region where according to our measurements the low-pressure isotherm feature is present. The most likely explanation is that a low-pressure substep was also present in the previous study, and that it was missed because of the low density of data points taken (indeed, there are hints of the presence of a substep at the appropriate coverage range for the lowest temperature reported in that study).

A number of possibilities exist regarding the origin of this feature. The simplest one is that adsorption occurs only on the grooves and the outer surface and that the low-pressure feature corresponds to adsorption on the grooves.[4] A second possibility is that adsorption occurs on the grooves and on defect-induced, large-diameter interstitial sites present on heterogeneous bundles, and on the outer surface of the individual tubes, and that the lower pressure step corresponds to the former two groups of sites.[9,16] Last, it is possible that some of the purified HiPco tubes may be open, and hence that the adsorption substep present at lower coverages corresponds to grooves, large interstices, *and* the interior of those tubes that are open and accessible.[10,12]

Comparing the experimental results with the simulations, we note first that, in the range of temperatures over which the experiments were performed, the simulations find that the lower pressure step is considerably broader than the higher pressure step. This is what the experimental results find, as well. Additionally, the computer simulations find that for CF_4 only three rows of atoms form on the surface of the SWNTs: two rows on the outer surface of the individual tubes and one row on the grooves. This is in excellent agreement with the coverages found at the top of the lower pressure step and at monolayer completion (the first being ~34% of the second, or very nearly a ratio of 1:3, just as in the simulations).

If some of the tubes were open and accessible, we would expect to find a higher fraction of high energy binding sites; that is, the lower pressure step should be larger than it is. We would also expect to find a higher value for the specific surface area. If we assume that the totality of the low-pressure step is the result of adsorption occurring on the inside of open tubes, we would obtain an accessible area (from the coverage at the top of the lower pressure step) of about 207 m^2/g. Simple geometric considerations lead to estimates for the inside area of the tubes on the order of 800 m^2/g.[18] This would indicate that, even if we were to (incorrectly) assume that the lower pressure step is entirely due to gas adsorbed inside open tubes, no more than about 26% of the tubes would be open. The ratio of the amount of Freon adsorbed on the outside external surface to that adsorbed on the grooves found in the simulations is 2:1; this is in very good agreement with our experimental findings for the ratio of the two substeps. Thus, if we consider the possibility that adsorption occurs on the grooves, and take into account the ratio found in the simulations, we are left with essentially zero adsorption taking place anywhere else on the bundles. (Zero adsorption inside the tubes is not unexpected: even though some tubes may be uncapped as a result of the purification process, access to their interior space will remain blocked unless appropriate steps are taken to remove the chemical functionalities that remain blocking the entries.[25,26] We did not heat our nanotubes to a sufficiently high temperature to achieve this.)

As a final possibility, we discuss the case that the HiPco nanotubes form heterogeneous bundles and have some large defect interstitial channels present. Because of its large molecular size, only the largest of the defect ICs would be accessible to CF_4. For smaller gases the simulations find that the binding energies on the large ICs are higher than or on the same order as those for the grooves. Hence any adsorption on the large defect-induced ICs in this case would appear as more adsorption occurring at coverages below that of the top of the lower pressure step. We find that the ratio of the coverage at the top of the lower pressure step to monolayer completion is close to 1:3. As our simulations show, this ratio can be explained in terms of adsorption on the grooves and outer sites. This indicates that any amount adsorbed in the large defect ICs is small when compared to the amount adsorbed on the grooves.

From this discussion it is clear the data available can be understood in terms of having all CF_4 molecules adsorbing on the outside surfaces of the nanotubes, and by having the lower pressure step correspond to adsorption on the grooves and the higher pressure one correspond to adsorption on the outer surface of individual tubes on the periphery of the bundle. While other possibilities have been considered (such as open-ended tubes or large diameter defect ICs), our results indicate the amount of adsorption corresponding to them is, at most, a small fraction of a monolayer.

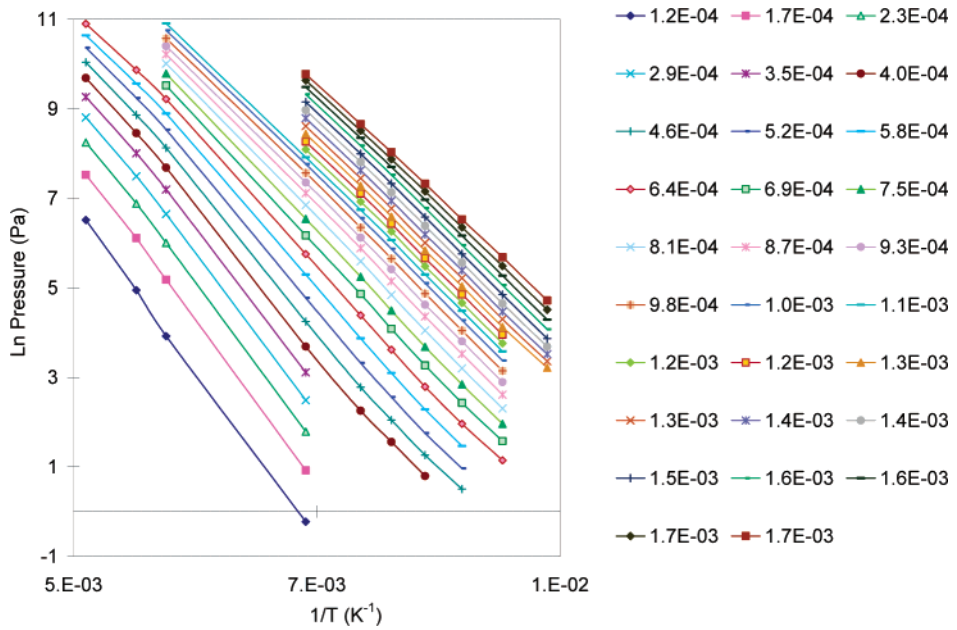

Figure 7. Natural logarithm of the pressure, for a fixed value of the coverage, plotted as a function of the inverse of the isotherm temperature. The coverages increase from left to right in the figure. The coverages (in moles) used are listed in the columns beside the figure.

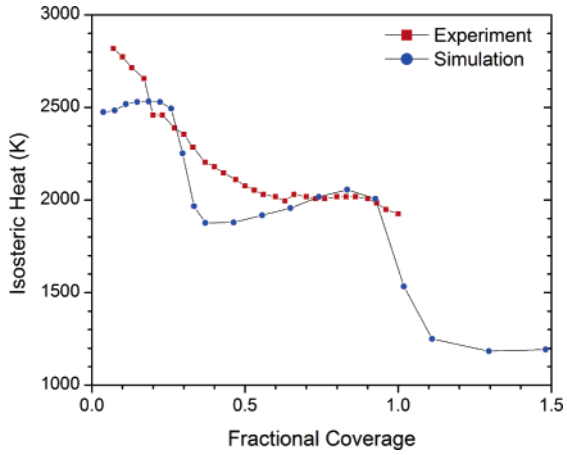

Figure 8. Isosteric heat as a function of fractional coverage. The experimental results were derived from the lines in Figure 7, while the simulated values were obtained from adsorption isotherms computed between 100 and 150 K.

Isosteric Heat of Adsorption. The isosteric heat of adsorption is the heat released by a molecule when it adsorbs on a surface. The isosteric heat of adsorption, q_{st}, can be determined from a set of isotherms at different temperatures, at different values of the coverage, N, from the relation[39]

$$q_{st} = -k_B\left(\frac{\partial \ln P}{\partial(1/T)}\right)_N$$

In practice the isosteric heat of adsorption can be obtained by plotting the value of ln P as a function of the inverse of the temperature, at fixed coverage. Figure 7 is just such a plot for coverages in the first layer. The isosteric heat is directly proportional to the slope of these curves.

The results for the isosteric heat as a function of the fractional coverage n (with respect to the monolayer coverage) are presented in Figure 8. The experimental data for the isosteric heat are a composite obtained from our different adsorption isotherm results. In the region between 0 and 1/5 layer the isosteric heat values were obtained from the low-coverage, high-temperature data (138 K < T < 207 K; see Figure 4); the values for higher coverages (above 0.4 monolayer) were obtained from the higher coverage portions of the low-temperature isotherms (99 K < T < 175 K; see Figure 5). The plateau present in the isosteric heat data corresponds to the higher pressure step in the isotherm. The value of the isosteric heat in this plateau region is 90% of the value found for this quantity on planar graphite. The previous study of CF_4 on SWNTs had found a slightly smaller value for this quantity, corresponding to 80% of the value on graphite.[5]

Isosteric heat values derived from the simulated isotherms with 100 K < T < 150 K are also shown in Figure 8. We note that for every value of the coverage the logarithm of the pressure as a function of the inverse of the isotherm temperature is a linear function, for temperatures in this range. Comparison with the experimental curve suggests that binding sites stronger than the external grooves may be occupied at low coverage. As has been shown in a recent study of CH_4 and Ar,[16] these are very likely to be interstitial spaces between four or more tubes that emerge as packing defects of bundles containing tubes with different diameters. However, the effect in this case is not as dramatic as it was in that previous work.[16] This difference is probably due to the larger size of the CF_4 molecules and the smaller size of the tubes used in the present experiments and simulations. For CF_4 the experimental values are only about 12% larger than the ones predicted by using the homogeneous bundle model in comparison with 40% differences found in that previous study.[16] Moreover, as discussed before, the ratio between the coverages of both steps in the experimental isotherms suggests that the fraction of molecules adsorbed in those sites is quite small. The agreement between the simulations and the experiments obtained here for the coverage dependence of the isosteric heat for the first layer of Freon is very good.

The binding energy for CF_4 on the strongest binding sites for this molecule on the nanotube bundles can be obtained from the determination of the isosteric heat of adsorption, q_{st}. If this quantity is determined at sufficiently low coverages (and temperatures) q_{st} is simply related to the binding energy through the expression

$$q_{st} = E_{binding} + \alpha kT \qquad (1)$$

where α is a constant that depends on the dimensionality of the adsorbed film (for a one-dimensional film, which is what we assume for CF_4 adsorbed on the grooves, $\alpha = 2$).[29] The low-coverage condition guarantees that there is no appreciable effect of gas−gas interactions, while the low-temperature regime allows one to assume that only the lowest transverse state is populated. In that case, $E_{binding} \approx V_{min} + \hbar\omega$, where V_{min} is the potential energy minimum and $\hbar\omega$ is the zero-point energy of the molecule confined in the external potential V. In the present case, $V_{min} = -2350$ K and $\hbar\omega \approx 50$ K.

We were not able to use low-coverage data from the lower temperature isotherms to compare with this theoretical result because the pressures corresponding to this region are too low for us to measure reliably in our setup. Even though one would expect that the low-coverage isosteric heat data obtained from the higher temperature isotherms would have some contribution from the occupation of higher energy states at those temperatures, plots of the particle density from the simulations show that the spread of the particles out of the groove is quite small even at $T = 200$ K. Thus, following the procedure outlined above, we obtained a binding energy value for CF_4 of 2400 K from the low-coverage, high-temperature isotherms. The experimental and simulated values are in excellent agreement.

For small adsorbates the values of the binding energy corresponding to the lower pressure step typically are between 1.6 and 1.7 times larger than those for the corresponding gas on the surface of planar graphite, while those for the higher pressure step are smaller (about 0.7 times the value on graphite).[1,2,4,6,8]

5. Conclusions

In conclusion, we have presented the combined results of computer simulations and adsorption isotherm investigations of CF_4 films on purified HiPco nanotubes. In addition to determining the features of the adsorption isotherm data, we also determined values for other thermodynamic quantities.

The simulations, conducted for homogeneous bundles of close-ended tubes, found two substeps in the first layer data: a low-pressure substep corresponded to adsorption on the grooves, and a higher pressure substep corresponded to adsorption on the outside surface of the tubes. The experimental measurements also found two substeps in the adsorption data. We considered several alternatives to explain the presence of these substeps. The very good agreement found between experiment and simulations for the values and characteristics of the isotherm features and for the coverage dependence of the isosteric heat, as well as the values obtained for the specific surface area, leads us to conclude that the experimental results are best described by the sequence seen in the simulations: most of the adsorption occurs on the outside surface of the bundle, with the low-pressure substep corresponding to adsorption on the grooves and the high-pressure substep corresponding to adsorption on the outside surface of the peripheral tubes.

Our experimental results were also extensively compared to previous experimental investigations for this system. The observed differences between them were noted and explained.

Acknowledgment. A.D.M. acknowledges the National Science Foundation for support through Grant DMR-0089713. Acknowledgment is made to the Donors of the American Chemical Society Petroleum Research Fund for partial support of this research (M.M.C.).

References and Notes

(1) Migone, A. D.; Talapatra, S. In *Encyclopedia of Nanoscience and Nanotechnology*; Nalwa, S., Ed.; American Scientific Publishers: Los Angeles, CA, 2004; Vol. 4, pp 749−767.
(2) *Adsorption by Carbons*; Tascon, J. M. D., Ed.; Elsevier Science: New York, 2006, in press.
(3) Calbi, M. M.; Cole, M. W.; Gatica, S. M.; Bojan, M. J.; Stan, G. *Rev. Mod. Phys.* **2000**, *73*, 857.
(4) Talapatra, S.; Zambano, A. J.; Weber, S. E.; Migone, A. D. *Phys. Rev. Lett.* **2000**, *85*, 138.
(5) Muris, M.; Dupont-Pavlovsky, N.; Bienfait, M.; Zeppenfeld, P. *Surf. Sci.* **2001**, *492*, 67.
(6) Muris, M.; Dufau, N.; Bienfait, M.; Dupont-Pavlovsky, N.; Grillet, Y.; Palmari, J. P. *Langmuir* **2000**, *16*, 7019.
(7) Stan, G.; Bojan, M. J.; Curtarolo, S.; Gatica, S.; Cole, M. W. *Phys. Rev. B* **2000**, *62*, 2173.
(8) Wilson, T.; Tyburski, A.; DePies, M. R.; Vilches, O. E.; Becquet, D.; Bienfait, M. *J. Low Temp. Phys.* **2002**, *126*, 403.
(9) Bienfait, M.; Zeppenfeld, P.; Dupont-Pavlovsky, N.; Muris, M.; Johnson, M. R.; Wilson, T.; DePies, M.; Vilches O. E. *Phys. Rev. B* **2004**, *70*, 035410.
(10) Du, W.-F.; Wilson, L.; Ripmeester, J.; Dutrisac, R.; Simard, B.; Denommee, S. *Nano Lett.* **2002**, *2*, 343.
(11) Fujiwara, A.; Ishii, K.; Suematsu, H.; Kataura, H.; Minawa, Y.; Suzuki, S.; Achiba, Y. *Chem. Phys. Lett.* **2001**, *336*, 205.
(12) Matranga, C.; Bockrath, B. *J. Chem. Phys.* **2005**, *109*, 4853.
(13) Kleinhammes, A.; Mao, S. H.; Yang, X. J.; Tang, X. P.; Shimoda, H.; Lu, J. P.; Zhou, O.; Wu, Y. *Phys. Rev. B* **2003**, *68*, 075418.
(14) Calbi, M. M.; Toigo, F.; Cole, M. W. *J. Low Temp. Phys.* **2002**, *126*, 179.
(15) Calbi, M. M.; Riccardo, J. L. *Phys. Rev. Lett.* **2005**, *94*, 246103.
(16) Shi, W.; Johnson, K. J. *Phys. Rev. Lett.* **2003**, *91*, 015504.
(17) Dresselhaus, M. S.; Williams, K. A.; Eklund, P. C. *MRS Bull.* **1999**, *24*, 45.
(18) Williams, K. A.; Eklund, P. C. *Chem. Phys. Lett.* **2000**, *320*, 352.
(19) Talapatra, S.; Migone, A. D. *Phys. Rev. Lett.* **2001**, *87*, 206106.
(20) Talapatra, S.; Rawat, D. S.; Migone, A. D. *J. Nanosci. Nanotechnol.* **2002**, *2*, 467.
(21) Talapatra, S.; Krungleviciute, V.; Migone, A. D. *Phys. Rev. Lett.* **2002**, *89*, 246106.
(22) Krungleviciute, V.; Heroux, L.; Talapatra, S.; Migone, A. D. *Nano Lett.* **2004**, *4*, 1133.
(23) Wilson, T.; Vilches, O. E. *Low Temp. Phys.* **2003**, *29*, 732.
(24) Teizer, W.; Hallock, R. B.; Dujardin, E.; Ebbesen, T. W. *Phys. Rev. Lett.* **1999**, *82*, 5305.
(25) Kuznetsova, A.; Yates, Jr., J. T.; Liu, J.; Smalley, R. E. *J. Chem. Phys.* **2000**, *112*, 9590.
(26) Kuznetsova, A.; Mawhinney, D. B.; Naumenko, V.; Yates, Jr., J. T.; Liu, J.; Smalley, R. E. *Chem. Phys. Lett.* **2000**, *321*, 292.
(27) Jakubek, Z. J.; Simard, B. *Langmuir* **2004**, *20*, 5940.
(28) Calbi, M. M.; Gatica, S. M.; Bojan, M. J.; Cole, M. W. *J. Chem. Phys.* **2001**, *115*, 9975.
(29) Calbi, M. M.; Cole, M. W. *Phys. Rev. B* **2002**, *66*, 115413.
(30) Kostov, M. K.; Calbi, M. M.; Cole, M. W. *Phys. Rev. B* **2003**, *68*, 245403.
(31) Dolle, P.; Matecki, M.; Thomy, A. *Surf. Sci.* **1980**, *91*, 271.
(32) Byl, O.; Kondratyuk, P.; Forth, S. T.; FitzGerald, A.; Chen, L.; Johnson, J. K.; Yates, Jr., J. T. *J. Am. Chem. Soc.* **2003**, *125*, 5889.
(33) Yim, W. L.; Byl, O.; Yates, J. T.; Johnson, K. J. *J. Am. Chem. Soc.* **2005**, *127*, 3198.
(34) Carbon Nanotechnologies, Inc., Houston, TX.
(35) Xiao Dong Hu, Carbon Nanotechnologies, Inc. Private communication.
(36) Gregg, S. J.; Sin, K. S. W. *Adsorption, Surface Area and Porosity*; Academic Press: London, 1967; pp 54−56.
(37) Rawat, D. S.; Heroux, L.; Krungleviciute, V.; Migone, A. D. *Langmuir* **2006**, *22*, 234.
(38) Lowell, S.; Shields, J. E. *Powder Surface Area And Porosity*; Chapman & Hall: London, 1991; pp 22−23.
(39) Dash, J. G. *Films on Solid Surfaces*; Academic Press: New York, 1975.